Microparticle formation by platelets exposed to high gas pressures – an oxidative stress response

Jasjeet Bhullar, Veena M. Bhopale, Ming Yang, Kinjal Sethuraman,
Stephen R. Thom

Department of Emergency Medicine, University of Maryland,
Baltimore, Maryland 21201

Microparticle formation by platelets

Key Words: singlet oxygen; S-nitrosylation; reactive nitrogen species; NADPH oxidase; focal adhesion kinase; filamentous actin

Address correspondence to: **Stephen R. Thom, M.D., Ph.D.,** Department of Emergency Medicine, University of Maryland, 655 W. Baltimore St., Bressler Research Building Room 4-013, Baltimore, MD 21201, Telephone: 410-706-8294, Fax: 410-328-8028

E-mail: sthom@smail.umaryland.edu

Highlights:

- High pressures of He, N_2, or Ar cause platelets to generate singlet O_2.
- Progressive production of reactive species involves NADPH oxidase.
- A cycle of actin polymerization occurs with nitric oxide synthase-2 activation.
- Actin S-nitrosylation and scaffold protein linkage trigger microparticles.

Abbreviations: Actin free barbed ends (FBE), focal adhesion kinase (FAK), microparticles (MPs), *n*-octyl -glucopyranoside (OG), NADPH oxidase (NOX), NADPH oxidase inhibitory peptide (NOX2ds), nitric oxide synthase (NOS), reactive oxygen species (ROS), singlet oxygen

sensor green (SOSG), thrombospondin-1 (TSP-1), Triton soluble, short filamentous actin (sF-actin), vasodilator-stimulated phosphoprotein (VASP).

Acknowledgements: This project was supported by Grants N00014-13-10613 and N00014-13-10614 from the Office of Naval Research, and R01-DK094260 from the National Institute of Diabetes and Digestive and Kidney Diseases,

ABSTRACT:

This investigation explored the mechanism for microparticles (MPs) production by human and murine platelets exposed to high pressures of inert gases. Results demonstrate that MPs production occurs via an oxidative stress response in a dose-dependent manner and follows the potency series N_2 > Ar > He. Gases with higher van der Waals volumes or polarizability such as SF_6 and N_2O, or hydrostatic pressure, do not cause MPs production. Singlet O_2 is generated by N_2, Ar and He, which is linked to NADPH oxidase (NOX) activity. Progression of oxidative stress involves activation of nitric oxide synthase (NOS) leading to S-nitrosylation of cytosolic actin. Exposure to gases enhances actin filament turnover and associations between short actin filaments, NOS, vasodilator-stimulated phosphoprotein (VASP), focal adhesion kinase (FAK) and Rac1. Inhibition of NOS or NOX by chemical inhibitors or using platelets from mice lacking NOS2 or the gp91phox component of NOX diminish generation of reactive species, enhanced actin polymerization and MP generation by high pressure gases. We conclude that by initiating a sequence of progressive oxidative stress responses high pressure gases cause platelets to generate MPs.

INTRODUCTION:

The focus of this investigation was to elucidate the mechanism for microparticles (MPs) production by platelets exposed to high gas pressures. MPs are 0.1 to 1 μm diameter membrane vesicles shed from all vascular cells in response to various stimuli [1]. MPs appear to serve as intercellular messengers because they may generate free radicals, contain cytokines or other signaling proteins, messenger RNA or microRNA [2, 3]. Healthy individuals have MPs, but levels are increased in a wide variety of inflammatory disorders; often by unclear mechanisms [1, 4-7]. We are interested in elucidating the pathophysiology for decompression sickness (DCS), a systemic disorder that occurs after tissues become super-saturated with one or more gases at high pressure.

Circulating MPs are elevated in experimental animals as well as humans in association with exposures to high gas pressures [8-14]. In a murine model, platelet and neutrophil-derived MPs have been shown to be the principal etiological agents causing tissue damage post-decompression [3, 15-17]. Interventions that diminish circulating MPs also abrogate decompression-induced tissue injury, and many of the same interventions reduce circulating MPs in human divers [18, 19]. MPs purified from decompressed mice can be injected into naïve mice and induce exactly the same pathological responses as does decompression [15-17].

We demonstrated that MPs generation by human and murine neutrophils occurs in response to a series of events involving reactive species production from NADPH oxidase (NOX) and type 2 nitric oxide synthase (NOS2), followed by cytoskeletal reorganization and activation of phospholipid transporters [20]. Notably, these events appeared to be initiated by singlet O_2, a highly reactive, diffusible, and long-lived electronically excited state of molecular O_2. The source

of singlet O_2 looked to be inert gas-O_2 collision complexes. Others have shown that singlet O_2 production during transient gas molecule collisions is influenced by molecular size of the collider species and gas polarizability [21, 22]. We found a dose-response for MPs production in neutrophils; N_2 and Ar were nearly equipotent and He markedly less so [20]. Collider molecules with van der Waals volumes above 35 ml/mol, such as SF_6 (van der Waals volume 46.8 ml/mol versus 15.8 for N_2) and those with relatively high polarizability such as N_2O (3.03×10^{24} cm^3 versus 1.74×10^{24} cm^3 for N_2) are less efficient, and these gases did not trigger MPs production [22-24].

Given the importance of platelets in DCS injury, we are interested in evaluating whether they generate MPs by a mechanism similar to that shown for neutrophils, as NOX and NOS2 are constitutively present, although NOS2 content is lower than NOS3 [25, 26]. MPs formation by platelets is known to be related to destabilization of the actin cytoskeleton [27]. Recent studies in megakaryocytes, as well as neutrophils, suggest that regulated MPs formation requires actin to polymerize and depolymerize in a coordinated fashion [28, 29].

METHODS:

Materials—Chemicals were purchased from Sigma-Aldrich unless otherwise noted. Compressed gases were purchased from Air Products and Chemicals, Inc. (Allentown, PA). NADPH oxidase inhibitory peptide (NOX2ds), which selectively inhibits the interaction between NOX2 and p47phox, with the sequence NH3-CSTRVRRQL-CONH2, and Scrmb-NOX2ds, a control scrambled amino acid peptide with sequence NH3-CLRVTRQSR-CONH2, were purchased from American Peptide Co. (Sunnyvale, CA). Edaravone (3-methyl-1-phenyl-2-pyrazolin-5-one) was purchased from Tocris Bioscience, Inc.. *N*-[6- (Biotinamido) hexyl]-3'-(2'-pyridyldithio) propionamide (biotin-HPDP) (catalogue no. 21341), neutravidin beads (catalog number 29200) and nitrocellulose membrane (catalog number LC2000) for immunoblotting were

purchased from Thermo Fisher Scientific. Antibodies to biotin (catalogue no. B3640) and actin (catalogue no. A2066) were purchased from Sigma. Polymorpho-prep was purchased from Axis Shield (catalogue no. 1114683, Oslo, Norway. NOS2 antibody (catalogue no.610431); VASP (catalogue no. 610448)**,** FAK (catalogue no. 610087), annexin V-conjugated FITC (catalogue no. 556419) and annexin-binding buffer solution (catalogue no. 556454) were purchased from BD Biosciences (San Jose, California). Anti-Rac1 (catalogue no. 05389) antibody was purchased from Millipore Corp. Singlet oxygen sensor green probe (SOSG) was purchased from Molecular Probes, Invitrogen.

Animals—Mice (*Mus musculus*) were purchased from Jackson Laboratories, Bar Harbor, ME, fed a standard rodent diet and water *ad libitum*, and housed in the university animal facility. A colony of NOS2 and gp91*phox* knock-out mice was maintained from breading pairs purchased from Jackson Laboratories. Animals (total use 68 wild type, 14 NOS2 and pg91*phox* KO mice) were anaesthetized by intraperitoneal administration of ketamine (100 mg/kg) and xylazine (10 mg/kg), skin was prepared by swabbing with Betadine, and blood was obtained by cardiac puncture into heparinized syringes.

Isolation of platelets and exposure to various agents—Heparin-anticoagulated blood was obtained from four non-SCUBA diving healthy volunteers from the University community (2 men, 2 women 42 $\pm$ 2 years old) using standard procedures. These individuals had taken no aspirin or other non-steroidal agents, or alcohol for the prior 48 hours. Murine and human platelets were isolated from heparinized blood using a published protocol [30]. Blood was made to a volume of 2.5 ml with wash buffer (PBS containing 1 mM $CaCl_2$, 1.5 mM $MgCl_2$, and 5.5 mM glucose) that was placed over 5 ml of Polymorphoprep plus 0.4 ml 1.5% NaCl in a 15-ml silicone-coated glass tube and centrifuged at 375 g for 30 min. The platelet-rich plasma was isolated and spun down at 1500g for 10 mins. The supernatant was discarded, and cell pellets

were resuspended in wash buffer at a concentration of 3 x 10^8/ml. Isolated human or mouse platelets (3 x 10^6/sample) were exposed at room temperature to either air at atmospheric pressure (100 kPa) or air plus partial pressures of He, N_2, Ar, N_20 or SF_6 up to 690 kPa following published procedures [20]. The standard procedure was to deposit samples in test tubes containing a magnetic stir bar, place them in stainless steel cylinders, apply gas pressure and stir constantly until decompressed at indicated times. Hydrostatic pressure as a control manipulation was achieved by placing platelet suspensions held in closed plastic syringes within the steel cylinders so that pressure could be applied to the sample via the plunger with no gas phase exposure.

The general approach to the study with the sequence of biochemical investigations is shown in Supplemental Figure 1. Initial MPs production studies were done with human platelets and then with murine platelets. Murine platelets from wild type and KO mice were used for all mechanistic investigations. Where indicated in the text, inhibitors were present in cell suspensions during gas exposures as follows: 1mM 1400 W (NOS2 inhibitor), 10µM NOX2ds (NOX inhibitor) or a scrambled sequence control peptide to NOX2ds (sc-NOX2ds), 5 µM cytochalasin D, 1 µM edaravone or 3 mM ascorbic acid. In some studies after gas exposures cell suspensions were exposed for 5 min to UV light from a 200-watt mercury vapor lamp.

MP enumeration and platelet degranulation by flow cytometry— Platelets were exposed to air or high pressures and after various intervals of time fixed using a Caltag Reagent A fixation medium (Invitrogen). Samples were centrifuged at 15,000 x *g* for 30 min to pellet platelets. Thereafter, samples containing supernatant were labeled with Annexin V FITC (Invitrogen) for 30 minutes in the dark before analysis. Flow cytometry was performed with an eight-color, triple laser MACSQuant (Miltenyi Biotec Corp., Auburn, CA) using the manufacturers' acquisition software. All reagents and solutions used for MP analysis were sterile and filtered using 0.1-µm

filter (Millipore, Massachusetts). Both forward scatter and side scatter were set at logarithmic gain. As an internal control, beads of various diameters (0.3 µm (Sigma), 1.0µm, and 3.0µm (Spherotech, Inc., Lake Forest, IL)) were incorporated for size measurements and were used before each experiment. Annexin V-positive particles with diameters from 0.1 to 1µm were considered as MPs. Analysis involved establishing true-negative controls by a fluorescence-minus-one analysis. An example of flow data patterns is shown in Figure 1.

Platelet activation was assessed by staining samples with CD41 and included fluorescent micro-beads with diameters of 3 and 5 µm in suspensions. Platelets were identified as particles between these micro-bead size limits that were CD41-positive and surface expression of CD62P and thrombospondin-1 (TSP-1) quantified as described in published procedures [13]. The fraction of platelets exhibiting fluorescence over the baseline following our standard fluorescence-minus-one analysis was used to quantify differences in activation between air-exposed and air + gas pressure exposed platelets.

Singlet oxygen detection— Singlet O_2 was assayed using singlet O_2 sensor green (SOSG) as the primary probe, with additional confirmation based on an assay involving use of 9,10-diphenylanthracene (DPA) as a singlet O_2 chemical trap [31, 32]. Platelet suspensions were incubated with SOSG at 1mM concentration and kept in dark for 30 minutes to allow uptake of the probe before exposing the cells to high pressure gas. Later cells were exposed to air or air plus 690 kPa of He, N_2, or Ar and after decompression fluorescence was measured (excitation 480 nm, 535 nm emission) at intervals according to published methods [33]. Some suspensions were treated with 3mM ascorbic acid or 1µM Edaravone for 15 minutes before inert gas exposures where indicated.

The DPA method for singlet O_2 detection was described by Steinbeck, *et al.* [31, 32]. A reagent film was produced by incubating 20 mg (~ 5 x 10^9) glass beads (0.178 – 0.297 mm diameter, Agsco Corp. Pine Brook, NJ) at room temperature in a 1 ml solution of dichloromethane containing 0.75 mg perylene and 7.5 mg DPA in the dark while being actively mix until all dichloromethane evaporated. Dried beads were stored at 4°C until use, at which time they were suspended in 1 ml PBS. Bead suspensions (200 µl) were combined with an equal volume of platelets (1 x 10^8/sample) for incubation in air or under elevated gas pressures for 30 minutes with constant stirring. Samples were then immediately place in 4.5 ml chloroform-methanol (2:1 ratio), the lower chloroform layer transferred and analyzed using a Varian-Cary 50 UV-Vis spectrophotometer to record the absorption spectrum between 500 and 300 nm wavelength. Using identical preparations exposed to air versus high gas pressure, singlet oxygen production was assessed as the difference between the 355 nm absorbance of native DPA versus lower absorbance caused by the DPA-endoperoxide following published methods [31, 32]. The only deviation from prior studies was that we were unable to reproducibly restore the native DPA after endoperoxide formation by evaporating the chloroform, re-suspending the precipitate in an equal volume of tetralin (1,2,3,4-tetrahydronaphthalene), and heating at 120°C for 1.5 hours. We found the precipitate formed with chloroform evaporation could not be reliably dissolved in tetralin so the post-heating spectrum sometimes only exhibited the background tetralin absorbance.

NOS activity assay in permeabilized platelets—Platelets were exposed to either air or 690 kPa N_2 for 30 mins and subjected to permeabilization using 0.2% *n*-octyl -glucopyranoside (OG), and NOS activity was assessed exactly as described previously [34]. Briefly, permeabilized cells (3x10^8/ml of wash buffer) were pre incubated with 40 µM *N*-hydroxy-L-arginine to inhibit arginase. After 10 min, 20mM L-[3H] arginine was added to cell suspensions

with or without 1 mM 1400W, and at intervals of time, 1 M trichloroacetic acid was added to quench the reaction. Cells were then pelleted by centrifugation at 5000 *g* for 5 min, washed three times with ethyl ether and passed through Dowex 50WX8 resin. L-[3H] Citrulline was eluted with two 0.5-ml washings with water and then analyzed using a scintillation counter.

Reactive species generation—Platelets suspensions were exposed to air or air plus 690 kPa of He, N_2, or Ar and then samples prepared with 5μM 2,7-dihydrodichlorofluorescein diacetate (DCF-DA), and fluorescence was monitored (504 nm excitation, 524 nm emission) according to procedures described previously [3].

Actin polymerization turnover as free barbed end production in permeabilized cells—Platelet suspensions were permeabilized using 0.2% *n*-octyl-b-glucopyranoside (OG) and then exposed to air or gas pressures as mentioned above, and actin polymerization was assayed as described before [35]. Suspensions were incubated for 10 seconds with 0.1 volume of OG buffer (60 mM PIPES, 25 mM Hepes (pH 6.9)), 10 mM EGTA, 2 mM $MgCl_2$, 4% OG, 10 μM phallacidin, 42 nM leupeptin, 10 mM benzamidine, and 0.123 mM aprotonin). After the incubation, 3 volumes of Buffer B (1 mM Tris (pH 7.0), 1 mM EGTA, 2 mM $MgCl_2$, 10 mM KCl, 5 mM β mercaptoethanol, and 5 mM ATP) were added. Actin polymerization was monitored for 30 minutes using a fluorescence spectrometer (360 nm excitation, 405 nm emission) when 1μM pyrene-labeled rabbit skeletal muscle actin was added to the platelet suspension.

Cell Extract Preparation and Biotin Switch Assay—Platelets were exposed to air or air plus 690 kPa N_2, centrifuged at 1500 x g and resuspended in HEN buffer (250 mM Hepes, pH 7.7, 1 mM EDTA, 0.1 mM neocuproine), lysed and subjected to the biotin-switch assay as previously described [36].

Cytoskeletal protein analysis based on Triton solubility— Platelets were exposed to air or air plus 690 kPa N_2 for 30 mins and then suspended in a solution of 0.5 mM dithiobis succinimidyl propionate (DTSP) to cross-link sulfhydryl-containing proteins within a proximity of ~12 Å following published procedures [30]. Cell lysates were separated into Triton-soluble G-actin, short F-actin and Triton-insoluble protein fractions and subjected to electrophoresis in gradient 4–15% SDS-polyacrylamide gels, followed by Western blotting.

Protein and peptide analysis — Mass spectrometry (MS) and protein sequencing were done by the John Hopkins School of Medicine Mass Spectrometry and Proteomics core facility. Protein bands identified as containing biotin on Western blots were cut from the gel, digested by endoproteinase GluC (V8) enzyme and analyzed by liquid chromatography interfaced with tandem MS (LCMS/MS) using the single or multi-dimensional protein identification technology (MuDPIT). The raw data files were searched using Mascot against NCBI database with a cut off protein score of 70 which then were imported into the scaffold software. Protein identifications in scaffold are deemed significant based on the standard criteria of > 2 peptides identified from the same protein with individual peptide scores >95% confidence, probability score at 1% FDR and sub 3 ppm mass error.

Statistical Analysis—Results are expressed as the mean $\pm$ SE for three or more independent experiments. We used analysis of variance (ANOVA) using SigmaStat (Jandel Scientific, San Jose, CA) and Holm-Sidak test to compare data. The level of statistical significance was defined as $p<0.05$.

RESULTS:

Microparticle production by platelets: Platelets from healthy human volunteers generated MPs when exposed to high pressure N_2 in a dose-dependent manner, whereas hydrostatic pressure (no gas phase) had no significant effect compared to control (air at ambient pressure) (Figure 2). There were MPs present in the platelet suspension at the start of the incubation. This number did not change with incubations for as long as 4 hours. The MPs count in the control samples reflects the number of MPs at 30 minutes after isolation to allow direct comparison to the samples exposed to high gas pressures.

Murine platelets responded to gas pressure in a comparable manner to human platelets (Table 1), and the potency of alternative gases was determined (Figure 3). Hydrostatic pressure and application of gas pressure using N_2O or SF_6 had no significant effect. MPs production was greatest with N_2, less with Ar, and lower still with He. There was no further elevation in MPs among platelet samples incubated for longer than 30 minutes under gas pressure or if samples were decompressed and left standing at ambient pressure for up to 4 hours (data not shown).

Platelets exposed to air versus air + 690 kPa N_2 were used to explore the mechanism for MPs generation. In these studies, platelets from knock-out mice lacking the gp91phox component of NOX or NOS2 were used, and results compared against platelets from wild type mice; as well as platelets from wild type mice incubated in the presence of specific chemical inhibitors (Table 2). The data indicate that NOS2 and NOX are required for MPs generation, as is actin turnover which is inhibited by cytochalasin D.

Singlet oxygen generation: High pressure SF_6 and N_2O do not generate singlet O_2 based on prior studies [20], and platelets incubated with edaravone or ascorbic acid, agents capable of quenching singlet O_2, failed to generate MPs when exposed to 690 kPa N_2 (Table 2). To more

directly assess whether gases generate singlet O_2, murine platelets were loaded with singlet oxygen sensor green (SOSG). Fluorescence measurements of samples immediately after 30 minute incubations versus prior to the incubations showed an increase of 254.7 $\pm$ 2.2 (n=6) fluorescence units for air-exposed and 652.2 $\pm$ 3.7 (n=6, $p<0.05$) fluorescence units for air + 690 kPa N_2 exposed samples. Measurements were not possible during the high pressure exposure, but the increased rate of fluorescence persisted when samples were assayed following decompression, as shown in Figure 4. Table 3 shows the progressive increase with 690 kPa He, N_2 and Ar. However, if platelets from mice lacking gp91phox were used, no significant increase in fluorescence occurred due to gas exposure. Fluorescence rate in the presence of air (control) was similar to wild type platelets, 9.0 $\pm$ 0.2 units/min (n=3) and virtually the same after exposure to air + 690 kPa N_2, 9.2 $\pm$ 0.7 (n=3, NS versus control).

As an alternative approach to confirm whether platelets generated singlet O_2 under high gas pressure, suspensions were incubated with DPA-coated glass beads while exposed to air (control) or air + 690 kPa N_2. Representative absorbance spectra are shown in Figure 5, where presence of the DPA-endoperoxide can be discerned as a reduction in 355 nm absorbance. We found no significant endoperoxide formation in air-exposed platelet preparations. Endoperoxide formation by high gas pressure was estimated to be 0.63 $\pm$ 0.14 (n=8, $p<0.05$) nmol/ 1 x 10^6 platelets using the change in 355 nm absorbance and the ratio of post- versus pre-exposure 438 nm absorbance (internal standard) as described by others [31, 32].

NOS activation by N_2: NOS activity was monitored as [^{3}H] citrulline production by platelets with or without co-incubation with 1400W. Consistent with the impact of enzyme inhibitors and results with NOS2 KO mouse platelets, gas pressure was found to activate NOS (Figure 6).

NOX activation by N_2: Reactive species production was monitored after platelets were incubated with membrane permeable DCF-DA (Figure 7). While DCF is known to react with a relatively wide variety of reactive species, we interpret the increase in fluorescence as occurring due to NOX activation because an enhanced rate of fluorescence did not occur when platelets were co-incubated with NOX2ds, as shown, and no elevation in fluorescence rate occurred with platelets from gp91phox KO mice (rate was comparable to air-exposed control at 55.4 $\pm$ 0.3 arbitrary units/min, n=3). We also found that co-activation of NOS2 was required for NOX activation. DCF fluorescence with platelets incubated with air + 1 mM 1400W was comparable to air-only samples in Figure 7, 45.1 $\pm$ 1.7 arbitrary units/min, n=4, and with air + 690 kPa N_2 + 1400W the slope was 45.6 $\pm$ 5.5 units/min, n=4 (NS). Similarly, platelets from NOS2 KO mice did not exhibit an enhanced rate of fluorescence when incubated with air + 690 kPa N_2 (51.8 $\pm$ 3.4 units/min, n=3, NS).

Role of the cytoskeleton in platelet MPs formation: A role for actin turnover for MPs production was discussed in Introduction, and as shown in Table 1, MPs formation in the presence of air + 690 kPa N_2 was inhibited by 5 µM cytochalasin D. Consistent with these findings, actin turnover monitored as formation of actin free barbed ends (Figure 8) was markedly increased by N_2 pressure and the effect abrogated by 1400W and NOX2ds.

Actin S-nitrosylation: Given that both NOX and NOS activity are required for gas-mediated MP production suggests a requirement for reactive species generated by interactions between nitric oxide ($^{\bullet}NO$) and reactive oxygen species (ROS). Therefore, we sought evidence for *S*-nitrosylation of platelet proteins by the biotin-switch assay, which covalently adds a disulfide linked biotin to the labile *S*-nitrosylation sites on proteins. Mouse platelets were exposed to air (control) and air + 690 kPa N_2 and Western blotting was performed on lysates probing for

biotinylated proteins (Figure 9). Prominent bands at ~71, 43 and 28 kDa were cut from gels and subjected to amino acid sequencing. The 71 kDa band was tentatively identified as cytoskeletal keratin type II, 43 kDa band as cytoskeletal actin, and the 28 kDa band as apolipoprotein E precursor. Protein loading is shown by probing for actin. We were especially interested in S-nitrosylated actin due to high pressure N_2, and we found it to be significantly reduced if platelets were co-incubated with 1400W, NOX2ds, or exposed for 5 mins to UV light, which photo-reverses *S*-nitrosylated cysteine, prior to biotin-switch assay (Table 4).

Protein associations with cytoskeletal actin: Because actin turnover appears to be essential for MP production based on the inhibitory effect of cytochalasin D, we were interested in evaluating associations of cytoplasmic actin with proteins known to play a role in turnover dynamics. After exposure to air or air + 690 kPa N_2, mouse platelets were incubated with the membrane permeable protein cross-linker DTSP and lysed after 30 minutes incubation at room temperature. Cell lysates were separated into Triton soluble G-actin, short filamentous (sF-) actin, and Triton-insoluble F-actin fractions and subjected to Western blotting. These were analyzed looking for differences in protein band densities relative to actin. A representative blot of the sF-actin fraction is shown in Figure 10 and quantitative changes for all three actin fractions are outlined in Table 5. There were marked elevations in protein associations in sF-actin fraction of the N_2 exposed platelets in comparison to the air control.

Platelet activation: We were interested in whether exposure to high gas pressure would cause overt platelet activation assessed by an increase membrane surface expression of CD62P and thrombospondin-1 (TSP-1) from α-granules. Platelets were exposed to air or air + 690 kPa N_2 for 30 minutes, then analyzed by staining the membrane surface with fluorophore-conjugated antibodies to CD62P and TSP-1. As shown in Table 6, no significant differences were found

between groups, leading to the conclusion that degranulation was not triggered by exposure to high gas pressure.

DISCUSSION:

Our results demonstrate that MPs production by mouse and human platelets exposed to high pressures of He, N_2 or Ar occurs in a dose-dependent manner in response to oxidative stress. The mechanism appears similar to that previously reported for gas pressure-induced MPs production by neutrophils [20]. Differences from the prior study with neutrophils include finding that MPs generation only persists for 30 minutes, whereas murine neutrophils will generate MPs for as long as 4 hours following just a 30 minute gas exposure, and the requirement of NOX activity for singlet O_2 generation. In the previous report we did not perform studies with cells from gp91*phox* KO mice, as our prime focus was an assessment of how chemically inert gases might trigger oxidative stress. There is, of course, precedence for chemically inert gases to have a biological effect – narcosis. In the classical theory, narcotic potency is based on molecular size and lipid solubility (oil-water partition coefficient). This process is not operating for MPs production because SF_6 exhibits a narcotic potency approximately 8.5-fold greater than N_2 whereas that for N_2O is 39-fold [37].

Results from this and our prior study indicate that a complex set of events is required for high pressure gases to stimulate MPs production, and these include activation of NOX and NOS2. Absence of an effect with SF_6 and N_20 supports a role for singlet O_2 as these gases do not generate this excited species under high pressure [20]. Inhibition of MPs formation by edaravone and ascorbic acid is also consistent with a role for singlet O_2, although these agents have non-specific effects. The sensitivity and specificity of SOSG for singlet O_2 has been evaluated [38, 39]. We used DPA endoperoxide detection as an independent method for

showing singlet O_2 production. It should be pointed out, however, that the DPA technique could only detect reactive species that escaped to the surrounding medium. Although not well known, singlet O_2 can be produced by spontaneous dismutation of superoxide generated by NOX and xanthine oxidase, as well as direct addition of potassium superoxide to water [31, 40-42]. Technical challenges are present for sensitive and specific assays of singlet O_2. There also is the problem that superoxide can be both source of singlet O_2 and an efficient quencher, although the chemistry described requires quite high superoxide concentrations [41, 43]. Given the requirement for NOX activity in the present study, it appears that high pressures of N_2, Ar and He can enhance singlet O_2 generation from superoxide. An enhanced electron transfer from collision complexes similar to that shown to occur in atmospheric chemistry may explain this phenomenon [21, 22, 44].

Others have reported alterations of actin cytoskeleton by singlet O_2, which may be operating in the MPs-generation process [45]. Singlet O_2 has many biological targets [46, 47] and it can act directly or through the successive formation of various secondary oxidative species with much longer half-lives [48, 49]. Hence, the results do not conclusively indicate that singlet O_2, versus a myriad of alternative reactive species, is directly required to trigger MPs formation. Interactions between ·NO and ROS generate species capable of protein nitration and nitrosylation reactions [50, 51]. In this regard, there is a recent description of S-nitrosylated actin formation as a consequence of singlet O_2 in another system [52]. Protein S-nitrosylation, the coupling of a ·NO moiety to a cysteine thiol group, has emerged as a specific and reversible post-translational signaling mechanism. Regulation of platelet function has been reported to involve S-nitrosylation [53]; ·NO nitrosylates N-ethylmaleimide-sensitive factor to regulate α-granule secretion, and integrin $\alpha_{IIb}\beta_3$ function to inhibit aggregation [54, 55]. Our data show that S-nitrosylation reactions are required for MPs production by platelets exposed to high gas

pressure, but interestingly, we do not see generalized platelet activation manifested as α-granule mobilization and display of CD62P or thrombospondin on the membrane surface.

The results show that cytoskeletal interactions and actin turnover are required for MPs generation. Observations are consistent with reports by us and others showing that activation of NOX and NOS2 occur in association with cytoskeletal reorganization [20, 56, 57]. While we identified that NOS2 and NOX interact with filamentous actin in platelets, we sought to characterize a number of other proteins involved in actin polymerization. Initial actin polymerization is slow but can be accelerated by the presence of short actin filaments [58]. VASP has been documented as a major component in platelet actin dynamics [59], and has been shown to both bundle filaments and nucleate actin polymerization [60]. VASP exhibits higher affinity for S-nitrosylated actin than un-modified actin, and we speculate this is why S-nitrosylation accelerates MPs production [30]. Additionally, FAK has been reported to induce NOX activation [61], and we have previously shown that by linking NOS2 to filamentous actin FAK accelerates MPs formation by neutrophils [20]. Rho GTPases such as Rac1 are required to remodel the actin cytoskeleton and drive the spreading and aggregation of platelets [62]. Rac1 is the major isoform present in human and murine platelets, and Rac proteins are essential components of the NOX enzyme complex [63]. Our cross linking studies demonstrate that high gas pressures increase short filamentous actin association with all of these regulatory proteins: NOS2, VASP, FAK and Rac1.

In summary, the dose-response reflected by our study of six gases and hydrostatic pressure indicate that gas molecular characteristics determine whether platelets generate MPs. The graphical abstract depicts the sequence of events we surmise from the data. Formation of singlet O_2 as a consequence of gas interactions with superoxide from NOX activity appears

responsible for the initiation of events. NOS2 activity and production of reactive species that generate S-nitrosylated actin advance the sequence with consequent associations of regulatory and scaffold proteins. These events may be generalized as reflecting cytoskeletal instability, which can enhance phospholipid turnover [64, 65]. This cascade ultimately results in MPs production.

REFERENCES:

[1] A.K. Enjeti, L.F. Lincz, M. Seldon, Detection and measurement of microparticles: an evolving research tool for vascular biology., Semin Thromb Hemost 33 (2007) 771-779.

[2] S.F. Mause, C. Weber, Microparticles: Protagonists of a novel communication network for intercellular information exchange., Circ Res 107 (2010) 1047-1057.

[3] S.R. Thom, M. Yang, V.M. Bhopale, T.N. Milovanova, M. Bogush, D.G. Buerk, Intra-microparticle nitrogen dioxide is a bubble nucleation site leading to decompression-induced neutrophil activation and vascular injury., J Appl Physiol 114 (2013) 550-558.

[4] A.K. Enjeti, L.F. Lincz, M. Seldon, Microparticles in health and disease., Semin Thromb Hemost 34 (2008) 683-692.

[5] B. Hugel, M.C. Martinez, C. Kunzelmann, J.M. Freyssinet, Membrane microparticles: Two sides of the coin., Physiology 20 (2005) 22-27.

[6] S.R. Thom, M. Bennett, N.D. Banham, W.W. Chin, D.F. Blake, A. Rosen, N.W. Pollock, D. Madden, O. Barak, A. Marroni, C. Balestra, P. Germonpre, M. Pieri, D. Cialoni, P.-N.J. Le, C. Logue, D.S. Lambert, K.R. Hardy, D. Sward, M. Yang, V.M. Bhopale, Z. Dujic, Association of microparticles and neutrophil activation with decompression sickness., J Appl Physiol 119 (2015) 427-434.

[7] M.R. Sanborn, S.R. Thom, L.E. Bohman, S.C. Stein, J.M. Levine, T. Milovanova, E. Maloney-Wilensky, S. Frangos, M.A. Kumar, Temporal dynamics of microparticle elevation following subarachnoid hemorrhage., J Neurosurg 117 (2012) 579-586.

[8] R.V. Vince, L.R. McNaughton, L. Taylor, A.W. Midgley, G. Laden, L.A. Madden, Release of VCAM-1 associated endothelial microparticles following simulated SCUBA dives., Eur J Appl Physiol 105 (2009) 507-513.

[9] L.A. Madden, B.C. Chrismas, D. Mellor, R.V. Vince, A.W. Midgley, L.R. McNaughton, S.L. Atkins, G. Laden, Endothelial function and stress response after simulated dives to 18 msw breathing air or oxygen., Aviat Space Environ Med 81 (2010) 41-51.

[10] S.R. Thom, T.N. Milovanova, M. Bogush, V.M. Bhopale, M. Yang, K. Bushmann, N.W. Pollock, M. Ljubkovic, P. Denoble, Z. Dujic, Microparticle production, neutrophil activation and intravascular bubbles following open-water SCUBA diving., J Appl Physiol 112 (2012) 1268-1278.

[11] S.R. Thom, T.N. Milovanova, M. Bogush, M. Yang, V.M. Bhopale, N.W. Pollock, M. Ljubkovic, P. Denoble, D. Madden, M. Lozo, Z. Dujic, Bubbles, microparticles and neutrophil activation: Changes with exercise level and breathing gas during open-water SCUBA diving., J Appl Physiol 114 (2013) 1396-1405.

[12] J.M. Pontier, E. Gempp, M. Ignatescu, Blood platelet-derived microparticles release and bubble formation after an open-sea dive., Appl Physiol Nutr Metab 37 (2012) 1-5.

[13] D. Madden, S.R. Thom, T.N. Milovanova, M. Yang, V.M. Bhopale, M. Ljubkovic, Z. Dujic, Exercise before SCUBA diving ameliorates decompression-induced neutrophil activation., Med Sci Sports Exerc 46 (2014) 1928-1935.

[14] D. Madden, S.R. Thom, M. Yang, V.M. Bhopale, T.N. Milovanova, M. Ljubkovic, Z. Dujic, High intensity cycling before SCUBA diving reduces post-decompression microparticle production and neutrophil activation., Eur J Appl Physiol 114 (2014) 1955-1961.

[15] S.R. Thom, M. Yang, V.M. Bhopale, S. Huang, T.N. Milovanova, Microparticles initiate decompression-induced neutrophil activation and subsequent vascular injuries., J Appl Physiol 110 (2011) 340-351.

[16] M. Yang, T.N. Milovanova, M. Bogush, G. Uzan, V.M. Bhopale, S.R. Thom, Microparticle enlargement and altered surface proteins after air decompression are associated with inflammatory vascular injuries., J Appl Physiol 112 (2012) 204-211.
[17] M. Yang, P. Kosterin, B.M. Salzberg, T.N. Milovanova, V.M. Bhopale, S.R. Thom, Microparticles generated by decompression stress cause central nervous system injury manifested as neurohypophiseal terminal action potential broadening., J Appl Physiol 115 (2013) 1481-1486.
[18] M. Yang, V.M. Bhopale, S.R. Thom, Ascorbic acid abrogates microparticle generation and vascular injuries associated with high pressure exposure., J Appl Physiol 119 (2015) 77-82.
[19] M. Yang, O.F. Barak, Z. Dujic, D. Madden, V.M. Bhopale, J. Bhullar, S.R. Thom, Ascorbic acid diminishes microparticle elevations and neutrophil activation following SCUBA diving., Am J Physiol 309 (2015) R338-R344.
[20] S.R. Thom, V.M. Bhopale, M. Yang, Neutrophils generate microparticles during exposure to inert gases due to cytoskeletal oxidative stress., J Biol Chem 289 (2014) 18831-18845.
[21] B.F. Minaev, G.I. Kobzev, Response calculations of electronic and vibrational transitions in molecular oxygen induced by interaction with noble gases. , Spectrochimica Acta Part A 59 (2003) 3387-3410.
[22] M. Hild, R. Schmidt, The mechanism of the collision-induced enhancement of the radiative transitions of oxygen., J Phys Chem A 103 (1999) 6091-6096.
[23] A. Bondi, van der Waals volumes and radii., J Phys Chem 68 (1964) 441-451.
[24] CRC, Handbook of Chemistry and Physics, 70th edition, Lide, D.R. (Ed), CRC Press, Boca Raton, FL (1989).
[25] L.Y. Chen, J.L. Mehta, Further evidence of the presence of constitutive and inducible nitric oxide synthase isoforms in human platelets., J Cardiovasc Pharmacol 27 (1996) 154-158.
[26] J.L. Mehta, L.Y. Chen, B.C. Kone, P. Mehta, P. Turner, Identification of constitutive and inducible forms of nitric oxide synthase in human platelets., J Lab Clin Med 125 (1995) 370-377.

[27] S. Cauwenberghs, M.A.H. Feijge, A.G.S. Harper, S.O. Sage, J. Curvers, J.W. Heemskerk, Shedding of procoagulant microparticles from unstimulated platelets by integrin-mediated destabilization of actin cytoskeleton., FEBS Lett 580 (2006) 5313-5320.

[28] R. Flaumenhaft, J.R. Dilks, J.C. Richardson, E. Alden, S.R. Patel-Hett, E. Battinelli, G.L. Klement, M. Sola-Visner, J.E. Italiano, Megakaryocyte-derived microparticles: direct visualization and distinction from platelet-derived microparticles., Blood 113 (2009) 1112-1121.

[29] S.E. Headland, H.R. Jones, A.S. D'Sa, M. Perretti, L.V. Norling, Cutting-edge analysis of extracellular microparticles using ImageStream(X) imaging flow cytometry., Sci Rep 4:5237(doi: 10.1038/srep05237) (2014).

[30] S.R. Thom, V.M. Bhopale, D.J. Mancini, T.N. Milovanova, Actin S-nitrosylation inhibits neutrophil beta2 integrin function, J Biol Chem 283(16) (2008) 10822-34.

[31] M.J. Steinbeck, A.U. Khan, M.J. Karnovsky, Cellular production of singlet oxygen by stimulated macrophages quantified using 9,10-diphenylanthracene and perlene in a polystyrene film., J Biol Chem 268 (1993) 15649-15654.

[32] M.J. Steinbeck, A.U. Khan, M.J. Karnovsky, Intracellular singlet oxygen generation by phagocytosing neutrophils in response to particles coated with a chemical trap., J Biol Chem 267 (1992) 13425-13433.

[33] A. Gollmer, J. Arnbjerg, F.H. Blaikie, B.W. Pedersen, T. Breitenbach, K. Daasbjerg, M. Glasius, P.R. Ogilby, Singlet oxygen sensor green: Photochemical behavior in solution and in a mammalian cell., Photochem.& Photobiol. 87 (2011) 671-679.

[34] S.R. Thom, V.M. Bhopale, M. Yang, M. Bogush, S. Huang, T. Milovanova, Neutrophil Beta-2 integrin inhibition by enhanced interactions of vasodilator stimulated phosphoprotein with S-nitrosylated actin., J Biol Chem 286 (2011) 32854-32865.

[35] M. Glogauer, J. Hartwig, T.P. Stossel, Two pathways through Cdc42 couple the N-formyl receptor to actin nucleation in permeabilized human neutrophils., J Cell Biol 150 (2000) 785-796.

[36] S.R. Thom, V.M. Bhopale, J.D. Mancini, T.M. Milovanova, Actin S-nitrosylation inhibits neutrophil beta-2 integrin function., J Biol Chem 283 (2008) 10822-10834.
[37] A. Ostlund, D. Linnarsson, F. Lind, A. Sporrong, Relative narcotic potency and mode of action of sulfur hexafluoride and nitrogen in humans., J Appl Physiol 76 (1994) 439-444.
[38] C. Flors, M.J. Fryer, J. Waring, B. Reeder, U. Bechtold, P.M. Mullineaux, S. Nonell, M.T. Wilson, N.R. Baker, Imaging the production of singlet oxygen in vivo using a new fluorescent sensor, Singlet Oxygen Sensor Green., J Exp Botany 57 (2006) 1725-1734.
[39] H. Lin, Y. Shewn, D. Chen, L.R. Lin, B.C. Wilson, B. Li, S.F. Xie, Feasibility study on quantitative measurements of singlet oxygen generation using singlet oxygen sensor green., J Fluoresc 23 (2013) 41-47.
[40] F. Tanfani, R. Fiorini, E. Tartaglini, A. Kantar, M. Wozniak, J. Antosiewicz, E. Bertoli, A sensitive detection of neutrophil activation by fluorescence quenching of membrane inserted singlet oxygen probe., Biochem Mol Biol Intl 32 (1994) 1093-1099.
[41] E.J. Corey, M.M. Mehrotra, A.U. Khan, Water induced dismutation of superoxide anion generates singlet molecular oxygen., Biochem Biophys Res Commun 15 (1987) 842-846.
[42] A.U. Khan, Singlet molecular oxygen from superoxide anion and sensitized fluorescence of organic molecules., Science 168 (1970) 476-477.
[43] H.J. Guiraud, C.S. Foote, Chemistry of superoxide ion. III. Quenching of singlet oxygen., J Am Chem Soc 98 (1976) 1984-1986.
[44] B.F. Minaev, G.I. Kobzev, Response calculations of electronic and vibrational transitions in molecular oxygen induced by interaction with noble gases., Spectrochimica Acta Part A 59 (2003) 3387-3410.
[45] M. Maftoum-Costa, K.T. Naves, A.L. Oliveira, A.C. Tedesco, N.S. da Silva, C. Pacheco-Soares, Mitochondria, endoplasmic reticulum and actin filament behavior after PDT with chloroaluminum phthalocyanine liposomal in HeLa cells., Cell Biol International 32 (2008) 1024-1028.

[46] K.R. Weishaupt, C.J. Gomer, T.J. Dougherty, Identification of singlet oxygen as the cytotoxic agent in photoinactivation of a murine tumor., Cancer Res 36 (1976) 2326-2332.
[47] M. Ochsner, Photophysical and photobiological processes in the photodynamic therapy of tumors. , J Photochem and Photobiol 39 (1997) 1-18.
[48] C. Tanielian, R. Mechin, R. Seghrouchni, C. Schweitzer, Mechanistic and kinetic aspects of photosensitization in the presence of oxygen., Photochem.& Photobiol. 71 (2000) 12-19.
[49] A.D. Wright, C.L. Hawkins, M.J. Davies, Photo-oxidation of cells generates long-lived intracellular protein peroxides. , Fr. Radic. Biol. Med. 34 (2003) 637-647.
[50] L. Pecci, G. Montefoschi, A. Antonucci, M. Casta, M. Fontana, D. Cavallini, Formation of nitrotyrosine by methylene blue photosensitized oxidation of tyrosine in the presence of nitrite., Biochem Biophys Res Commun 289 (2001) 305-309.
[51] H. Ischiropoulos, S. Thom, A comparison of the biological reactivity of nitric oxide and peroxynitrite., in: L. Ignarro (Ed.), Nitric Oxide, Academic Press2000, pp. 83-89.
[52] M. Rodriguez-Serrano, D.M. Pazmino, I. Sparkes, A. Rochetti, C. Hawes, M.C. Romero-Puertas, L.M. Sandalio, 2,4-dichlorophenoxyacetic acid promotes S-nitrosylation and oxidation of actin affecting cytoskeleton and peroxisomal dynamics. , J Exp Botony 65 (2014) 4783-4793.
[53] C. Irwin, W. Roberts, K.M. Naseem, Nitric oxide inhibits platelet adhesion to collagen through cGMP-dependent and independent mechanisms: The potential mrole for S-nitrosylation., Platelets 20 (2009) 478-486.
[54] C.N. Morrell, K. Matsushita, K.A. Chiles, R.B. Scharpf, M. Yamakuchi, R.J. Mason, W. Bergmeier, J.L. Mankowski, W.M. Baldwin, N. Faraday, C.J. Lowenstein, Regulation of platelet granule exocytosis by S-nitrosylation., PNAS 102 (2005) 3782-3787.
[55] G.M. Walsh, M.D. Leane, N. Moran, T.E. Keyes, R.J. Forster, D. Kenny, S. O'Neill, S-nitrosylation of platelet alphaaIIbeta3 as revealed by Raman spectroscopy., Biochemistry 46 (2007) 6429-6436.

[56] R.P. Brandes, N. Weissmann, K. Schroder, Nox family NADPH oxidases in mechano-transduction: Mechanisms and consequences. , Antioxid Redox Signal 20 (2014) 887-898.
[57] Y. Su, S. Edwards-Bennett, M.R. Bubb, E.R. Block, Regulation of endothelial nitric oxide synthase by the actin cytoskeleton, Am J Physiol Cell Physiol 284(6) (2003) C1542-9.
[58] A.A. Lal, E.D. Korn, S.L. Brenner, Rate constants for actin polymerization in ATP determined using cross-linked actin trimers as nuclei. , J Biol Chem 259 (1984) 8794-8800.
[59] E.L. Bearer, Cytoskeletal domains in the activated platelet., Cell Motil Cytoskeleton 30 (1995) 50-66.
[60] E.L. Bearer, J.M. Prakash, R.D. Manchester, P.G. Allen, VASP protects actin filaments from gelsolin: an in vitro study with implications for platelet actin reorganizations. , Cell Motil Cytoskeleton 47 (2000) 351-364.
[61] A. Kasorn, P. Alcaide, Y. Jia, K.K. Subramanian, B. Sarraj, Y. Li, F. Loison, H. Hattori, L.E. Silberstein, W.F. Luscinskas, H.R. Luo, Focal adhesion kinase regulated pathogen-killing capability and life span of neutrophils via mediating both adhesion-dependent and -independent cellular signals., J Immunol 183 (2009) 1032-1043.
[62] O.J. McCarty, M.K. Larson, J.M. Auger, N. Kalia, B.T. Atkinson, A.C. Pearce, S. Ruf, R.B. Henderson, V.L. Tybulewicz, L.M. Machesky, S.P. Watson, Rac1 is essential for platelet lamellipodia formation and aggregate stability under flow. , J Biol Chem 280 (2005) 39474-39484.
[63] M.C. Dinauer, Regulation of neutrophil function by Rac GTPases., Curr Opin Hematol 10 (2003) 8-15.
[64] J.M. Freyssinet, F. Toti, Formation of procoagulant microparticles and properties. , Thromb Res 125 (suppl 1) (2010) S46-S48.
[65] O. Morel, L. Jesel, J.M. Freyssinet, F. Toti, Cellular mechanisms underlying the formation of circulating microparticles. , Arterioscler Thromb Vasc Biol 31 (2011) 15-26.

FIGURE LEGENDS:

Figure 1. Representative flow cytometry analysis of MPs. After forward (FSC-H) and side scatter (SSC-H) interrogation using 0.3, 1 and 3 µm diameter beads in buffer (box a), histograms are established (b). This allows evaluating a dot plot for particles (c) and selecting those with sizes between 0.3 and 1 µm (d). In separate analyses particles from platelet suspensions are evaluated using fluorophore-conjugated antibodies based on the fluorescence-minus-one (FMO) control test to establish positive staining for Annexin V. Box (e) shows the FMO selection area for MPs from a sample after air (control) exposure, box (f) shows MPs from a sample after exposure to air + 690 kPa N_2.

Figure 2: MP production by human platelets. MPs were evaluated in platelet suspensions after 30 minute exposures to air (control), air plus 186, 345, or 690 kPa of N_2 and 690 kPa of hydrostatic pressure. Data are mean ± SE, (n) indicate number of independent experiments, * indicates significantly different from the air control ($p<0.05$, ANOVA).

Figure 3: MP production by murine platelets. MP were counted in platelet suspensions after 30 minute exposures to air (control), 690 kPa of hydrostatic pressure, or air + 690 kPa He, Ar or N_2. Data are mean ± SE, (n) indicate number of independent experiments, * indicates significantly different from the air control ($p<0.05$, ANOVA), (a) indicates significantly different from all other samples.

Figure 4: Singlet oxygen sensor green (SOSG) fluorescence in platelet suspensions after gas exposure. Platelets incubated with SOSG were exposed to air or air + 690 kPa of N_2 for 30 minutes, then fluorescence monitored for 5 minutes. Where indicated, samples included 1 µM edaravone or 3 mM ascorbic acid. Data are mean fluorescence values at each time point for 3

independent studies as mean ± SE. All values for N_2, but not N_2 plus ascorbic acid or edaravone, are significantly different from air (control) ($p<0.05$ ANOVA).

Figure 5: Absorbance spectra of chloroform-extracted product from platelet suspensions incubated with glass beads coated with DPA- perylene. Air indicates control sample incubated in air for 30 minutes (solid line), N_2 sample was incubated with air + 690 kPa N_2 prior to extraction (dotted line). DPA exhibits a prominent absorbance at 355 nm whereas DPA-endoperoxide does not.

Figure 6: NOS activity. Data show the activity of NOS monitored as [^{3}H] citrulline production for murine platelets incubated with substrate [^{3}H] arginine and exposed to air, air + 690 kPa N_2 without or with 1 mM 1400 W. Data are mean ± SE for measurements at each time point using 3 to 5 independent samples* $p<0.05$ versus air (ANOVA).

Figure 7: DCF fluorescence: Murine platelets were exposed to air or air + 690 kPa N_2 for 30 minutes without or with 10 µM Nox2ds, then combined with 5µM DCF-DA and fluorescence monitored for the 15 minutes. Data are mean ± SE for measurements at each time point using 3 independent samples, * $p<0.05$ versus air (ANOVA).

Figure 8: Actin turnover assessed by free barbed ends (FBE) formation. Murine platelets were exposed to air or air + 690 kPa N_2 for 30 minutes and actin turnover assessed by adding 1µM pyrene-labeled rabbit skeletal muscle actin (see Methods). Where indicated platelets were co-incubated with 1 mM 1400 W or 10 µM NOX2ds during the initial air or air + N_2 exposure. Data are mean ± SE for measurements at each time point using 3 independent samples, * $p<0.05$ versus air (ANOVA).

Figure 9: Western blot showing biotinylated proteins. Murine platelets were exposed to air or air + 690 kPa N_2 for 30 minutes and cell lysates were prepared according to the biotin switch assay. A representative blot is shown.

Figure 10: Protein associations in the Triton soluble short F-actin fraction. Murine platelets were exposed to air or air + 690 kPa N_2 for 30 minutes, incubated with the membrane permeable protein cross-linker DTSP, lysed and the Triton soluble short-F actin fraction subjected to Western blotting. This image is one representative of three independent experiments. Quantitative data on relative band densities versus the actin band are shown in Table 4.

Table 1: Gas dose-dependency for MP production by murine platelets. MPs produced per murine platelet exposed to air or air + 186, 345, or 690 kPa of N_2, or air + 690 kPa N_2O or SF_6. Data are mean ± SE, (n) indicates number of independent experiments, * indicates significantly different from the air control ($p<0.05$, ANOVA).

Gas	**MPs/platelet x10^2**
Air	3.43 ± 0.27 (21)
+ 186 kPa N_2	5.28 ± 0.27 (3)
+ 345 kPa N_2	6.19 ± 0.77 (3) *
+ 690 kPa N_2	13.1 ± 0.31 (21)*
+ 690 kPa N_2O	3.12 ± 0.17 (3)
+ 690 kPa SF_6	3.08 ± 0.07 (3)

Table 2: MP production by murine platelets. Mouse platelets were exposed to air or air plus 690 kPa N_2 for 30 minutes and counts expressed as MPs/platelet x 10^2. Where indicated samples were incubated with 1 mM 1400 W (NOS2 inhibitor), 10 µM NOX2ds (NOX inhibitor) or scNox2ds (a scrambled sequence control peptide to NOX2ds), 5 µM cytochalasin D, 1 µM edaravone or 3 mM ascorbic acid. NOS 2 KO and gp91^{phox} KO indicate samples of platelets from mice lacking NOS2 and active NOX. All values are mean ± SE, (n) indicates number of independent trials, * indicates significantly different from control ($p<0.05$).

Agent	Air	N_2
PBS	3.43 ± 0.27 (21)	13.1 ± 0.78 (21) *
1400 W	3.58 ± 0.25 (8)	3.33 ± 0.70 (8)
Sc Nox 2ds	4.08 ± 0.34 (3)	12.6 ± 0.52 (6)*
Nox2ds	4.03 ± 0.51 (3)	5.2 ±1.05 (6)
Cytochalasin D	3.72 ± 0.21 (3)	4.17± 0.92 (3)
Ascorbic acid	3.60 ± 0.21 (3)	3.77 ± 0.15 (3)
Edavarone	3.53 ± 0.15 (3)	3.63 ± 0.23 (3)
NOS 2 KO	3.97 ± 0.48 (3)	3.46 ± 0.12 (3)
gp91^{phox} KO	4.02 ± 0.43 (4)	3.88 ± 0.52 (4)

Table 3: Potency for different gases to produce SOSG fluorescence. Data show singlet oxygen sensor green fluorescence increase/minute after platelets were expose for 30 minutes to air or air + 690 kPa He, Ar or N_2. Data represent mean ± SE for 3 independent experiments, * indicates $p<0.05$ vs air (control).

Gas	Fluorescence/min
Air	7.9 ± 0.2 (3)
Helium	20.5 ± 0.8 (3) *
Argon	46.0 ± 0.2 (3) *
Nitrogen	37.3 ± 0.1 (3) *

Table 4: SNO actin/βactin band density ratios. Data are the densities of the 42 kDa band on Western blots of lysates from cells exposed to air or air + 690 kPa N_2 for 30 minutes subjected to the biotin switch assay expressed as a ratio to the cytosolic actin band density of each preparation, and normalized to the ratio found for air-exposed platelets for each individual experiment. Platelets were incubated with buffer (PBS) only or with buffer plus 1mM 1400 W or 10μM NOX2ds during air/N_2 exposures. UV indicates cells exposed to UV light for 5 minutes after air/N_2 exposure. Data represent mean ± SE (n= number of independent trials; shown in parentheses), *p<0.05 versus PBS-air sample.

Agent	**Air**	**Air + 690 kPa N_2**
PBS	1.00 ± 0.00 (4)	2.39 ± 0.21 (4) *
1400W	0.75 ± 0.16 (3)	0.93 ± 0.18 (3)
Nox2ds	1.03 ± 0.03 (3)	1.24 ± 0.07 (3)
UV	0.93 ± 0.08 (3)	1.29 ± 0.03 (3)

Table 5: Protein associations assessed by DTSP cross-linking in sF-actin, G-actin, and Triton-insoluble actin fractions of platelets exposed to air (control) or for 30 min to air + 690 kPa N_2. Values are ratios calculated based on the band densities of the identified protein relative to the actin band density in each sample. Values are normalized to air-exposed control protein band ratios of individual experiments, thus values greater than 1.0 reflect increases in protein associations with actin, whereas values less than 1.0 indicate lower protein associations. Data are mean ± SE (n= number of independent trials; shown in parentheses), * reflects values significantly different from normalized air-exposed control values ($p<0.05$, ANOVA).

	NOS2/actin	**VASP/actin**	**FAK/actin**	**Rac1/actin**
s F-Actin 100 psi N_2	1.81 ± 0.07* (4)	1.62 ± 0.04* (3)	1.52 ± 0.03* (3)	1.41 ± 0.02* (3)
G-Actin 100 psi N_2	0.93 ± 0.02 (4)	1.11 ± 0.04 (3)	0.99 ± 0.04 (3)	1.03 ± 0.05 (3)
Triton-insoluble 100 psi N_2	1.07 ± 0.03 (4)	1.06 ± 0.04 (3)	1.05 ± 0.06 (3)	1.11 ± 0.03 (3)

Table 6. Platelet activation. Mouse platelets were exposed to air or air + 690 kPa N_2 for 30 minutes. Values indicate the percent of the platelet populations expressing CD62P and TSP-1 above the fluorescence-minus-one threshold for indicating positive staining. Data are mean ± SE for 4 independent measurements, values are not statistically significantly different.

Surface Marker	**Air**	**Air+ 690 kPa N_2**
CD62P	2.12 ± 0.41	1.90 ± 0.51
TSP	2.41 ± 0.61	1.63 ± 0.35

Graphical Abstract: The studies show that high pressures of N_2, Ar and He, but not N_2O, SF_6 or hydrostatic pressure (HP), will interact with NADPH oxidase (NOX) derived superoxide ($O_2^{\cdot-}$) to yield singlet oxygen (O_2^*). Subsequent interactions with NOS2 derived products result in actin S-nitrosylation (SNO-actin) that enhances cytoskeletal turnover ultimately causing microparticle (MPs) formation.

Figure 1

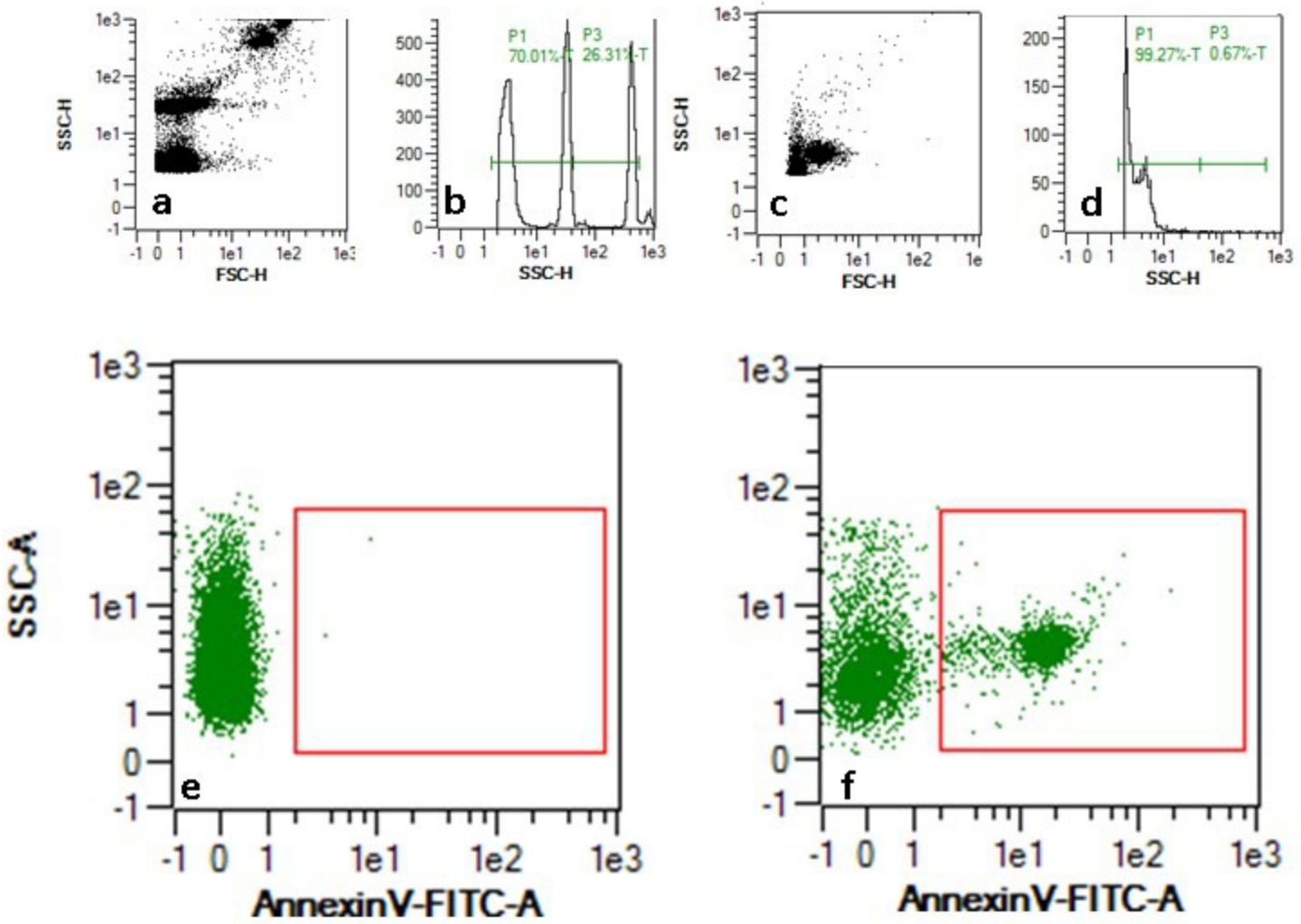
a
SSC-H
FSC-H
b
P1
70.01%-T
P3
26.31%-T
SSC-H
c
SSC-H
FSC-H
d
P1
99.27%-T
P3
0.67%-T
SSC-H
e
SSC-A
AnnexinV-FITC-A
f
AnnexinV-FITC-A

Figure 2

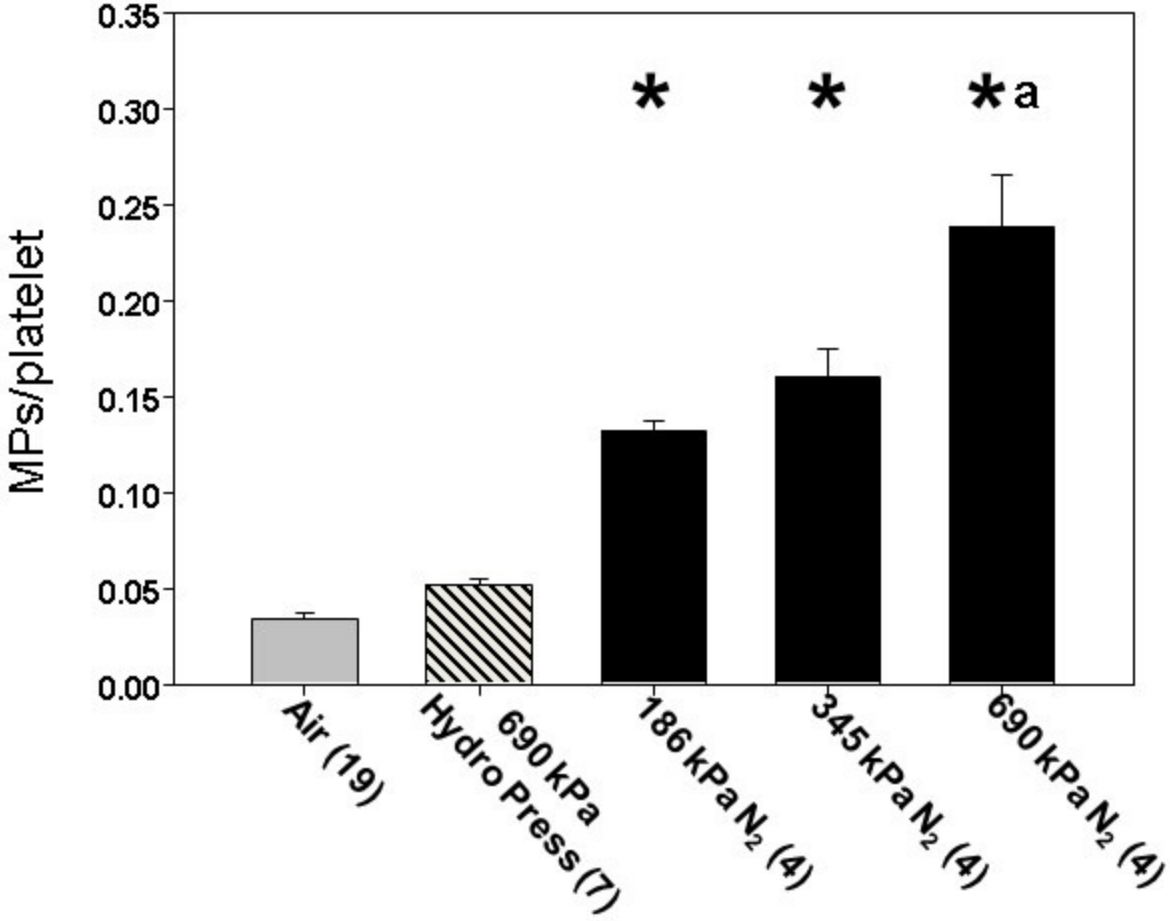
MPs/platelet
0.35
0.30
0.25
0.20
0.15
0.10
0.05
0.00
*
*
*a
Air (19)
Hydro Press (7)
690 kPa
186 kPa N2 (4)
345 kPa N2 (4)
690 kPa N2 (4)

Figure 3

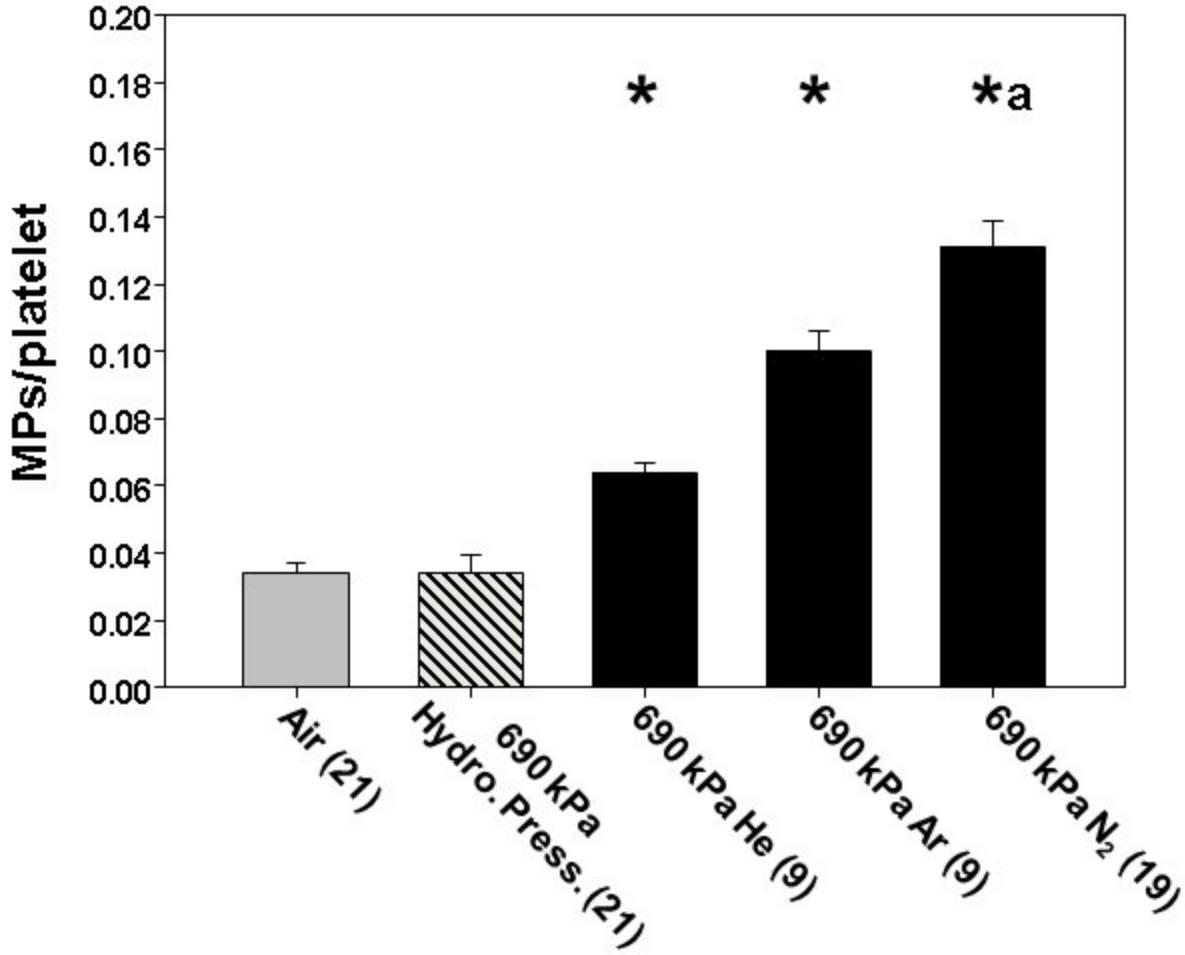
MPs/platelet
0.20
0.18
0.16
0.14
0.12
0.10
0.08
0.06
0.04
0.02
0.00
*
*
*a
Air (21)
690 kPa Hydro. Press. (21)
690 kPa He (9)
690 kPa Ar (9)
690 kPa N2 (19)

Figure 4

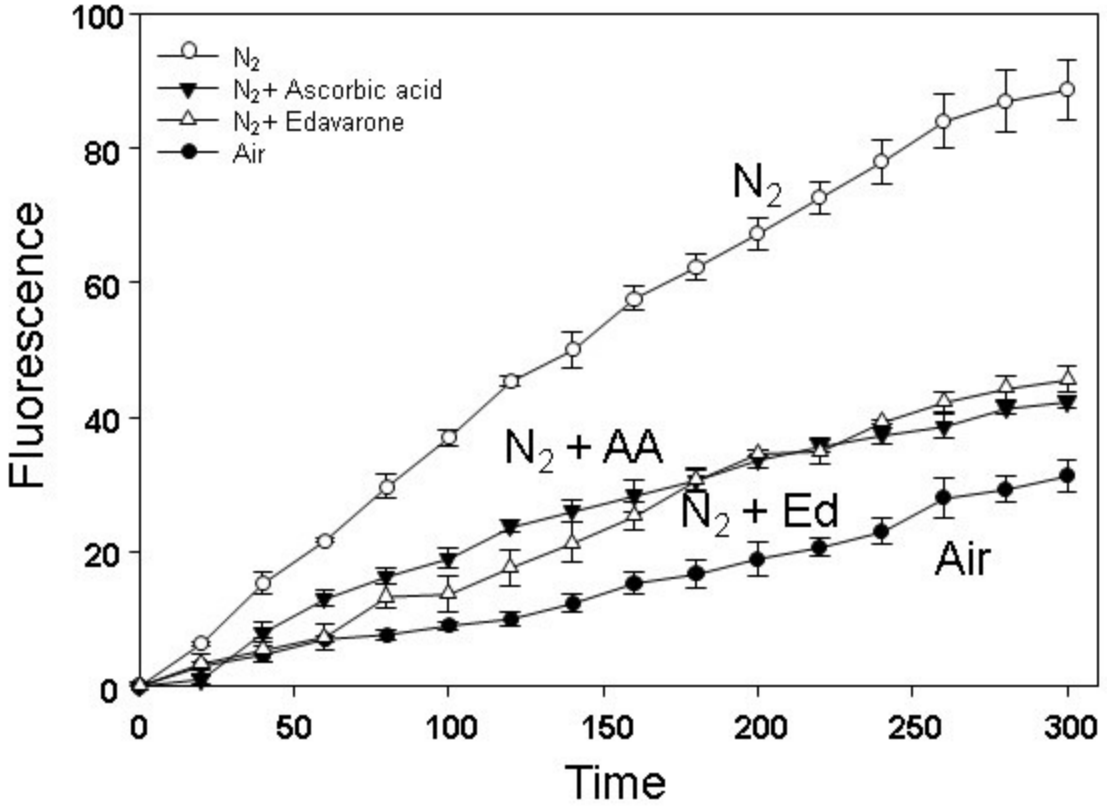
100
80
60
40
20
0
Fluorescence
0
50
100
150
200
250
300
Time
N2
N2+ Ascorbic acid
N2+ Edavarone
Air
N2
N2 + AA
N2 + Ed
Air

Figure 5

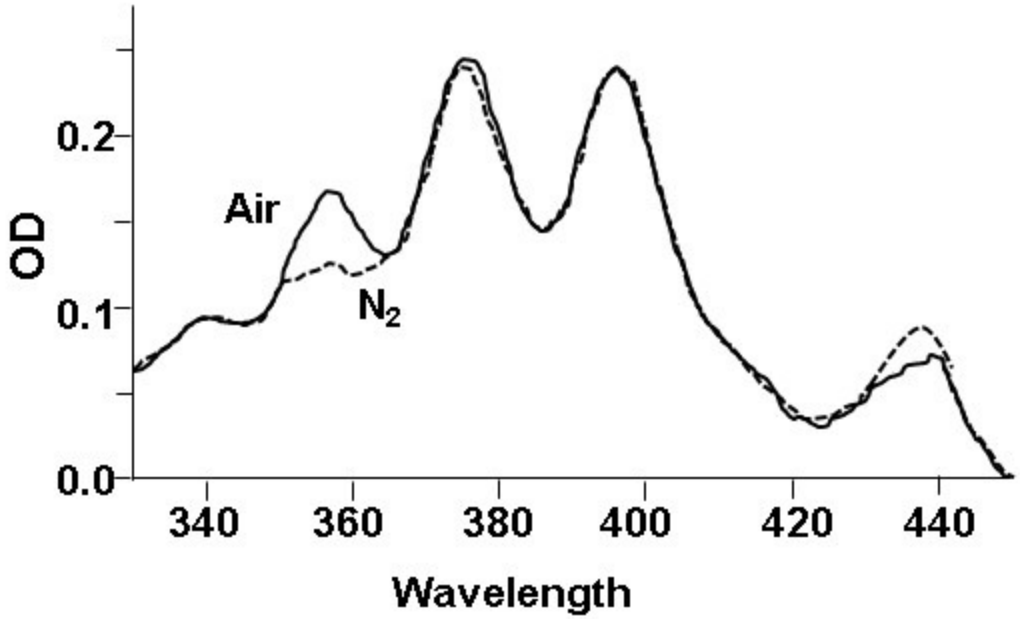

Figure 6

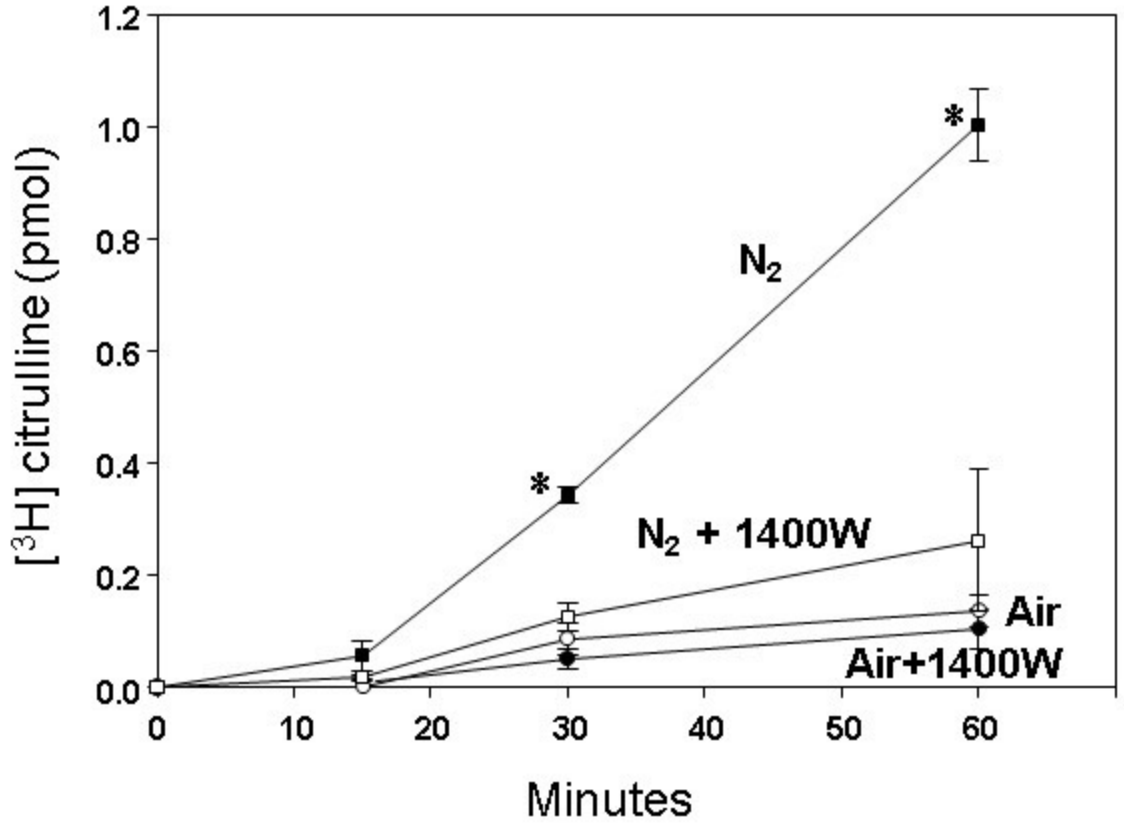
1.2
1.0
0.8
0.6
0.4
0.2
0.0
[3H] citrulline (pmol)
0
10
20
30
40
50
60
Minutes
*
*
N2
N2 + 1400W
Air
Air+1400W

Figure 7

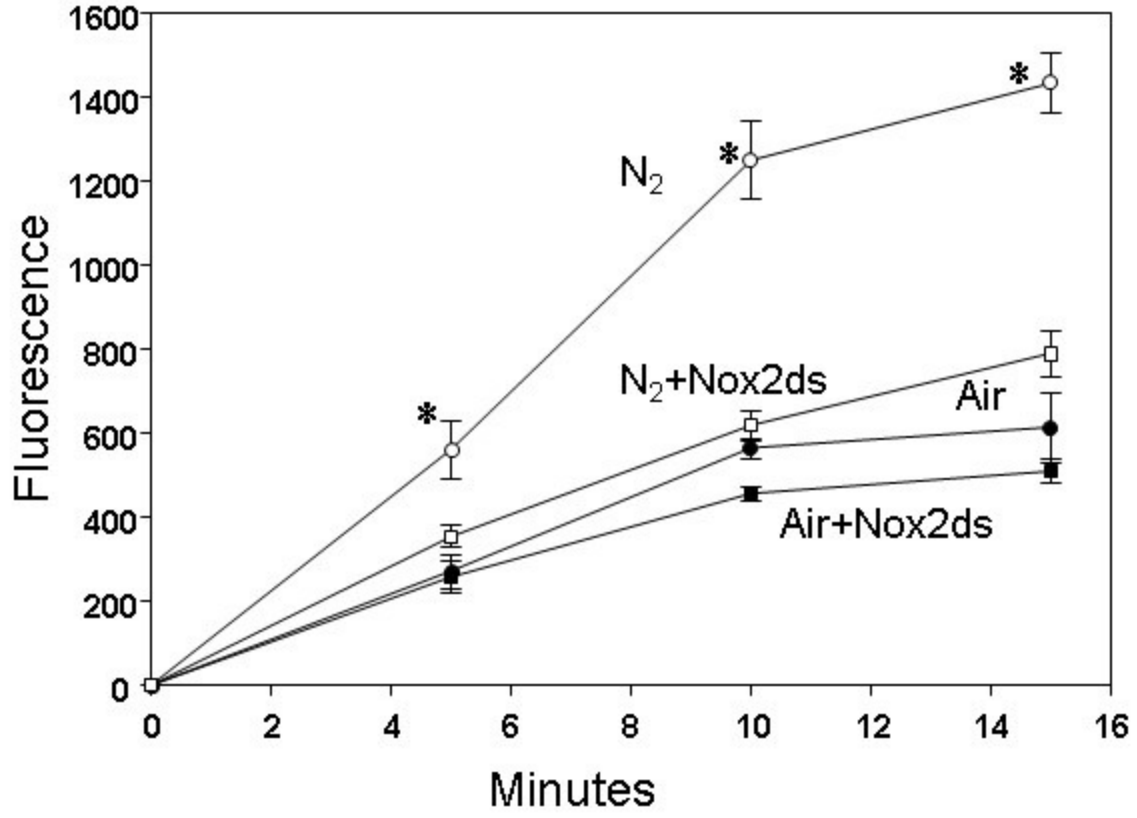
1600
1400
1200
1000
800
600
400
200
0
Fluorescence
0
2
4
6
8
10
12
14
16
Minutes
N2
N2+Nox2ds
Air
Air+Nox2ds
*
*
*

Figure 8

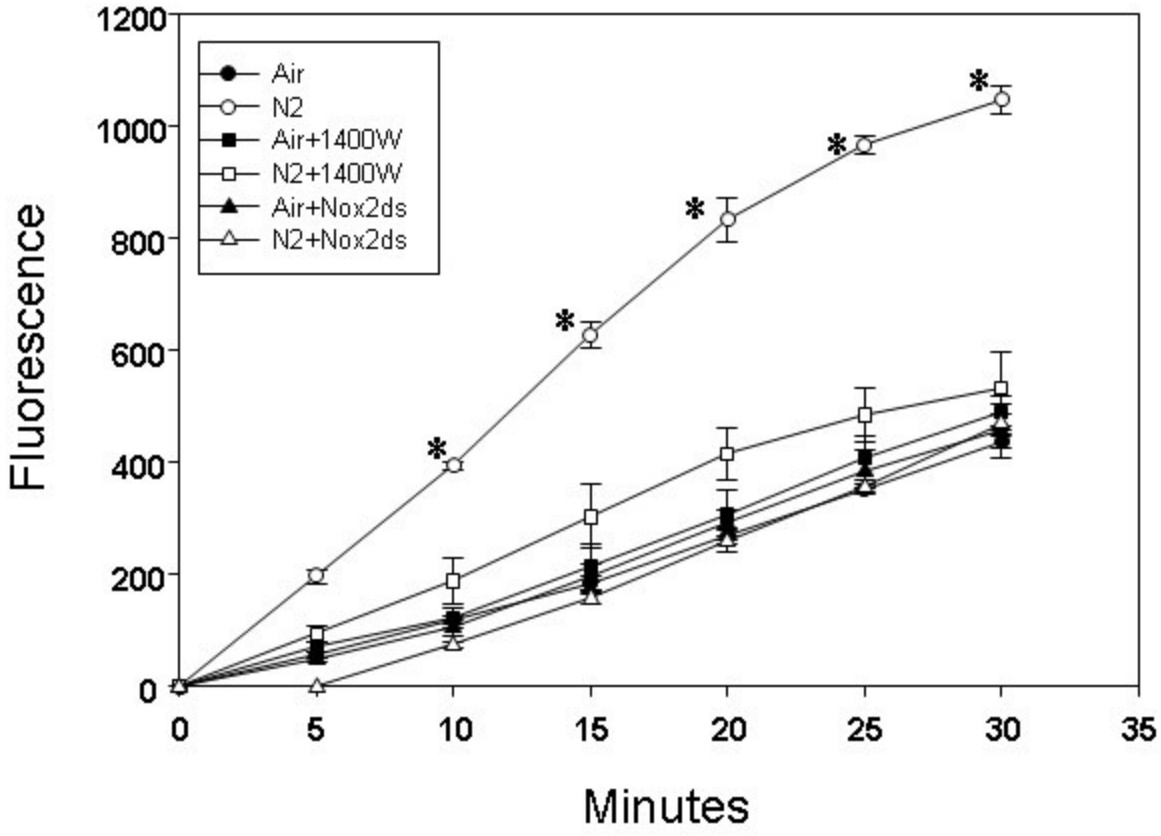
Air
N2
Air+1400W
N2+1400W
Air+Nox2ds
N2+Nox2ds
Fluorescence
Minutes
0
200
400
600
800
1000
1200
0
5
10
15
20
25
30
35
*
*
*
*
*

Figure 9

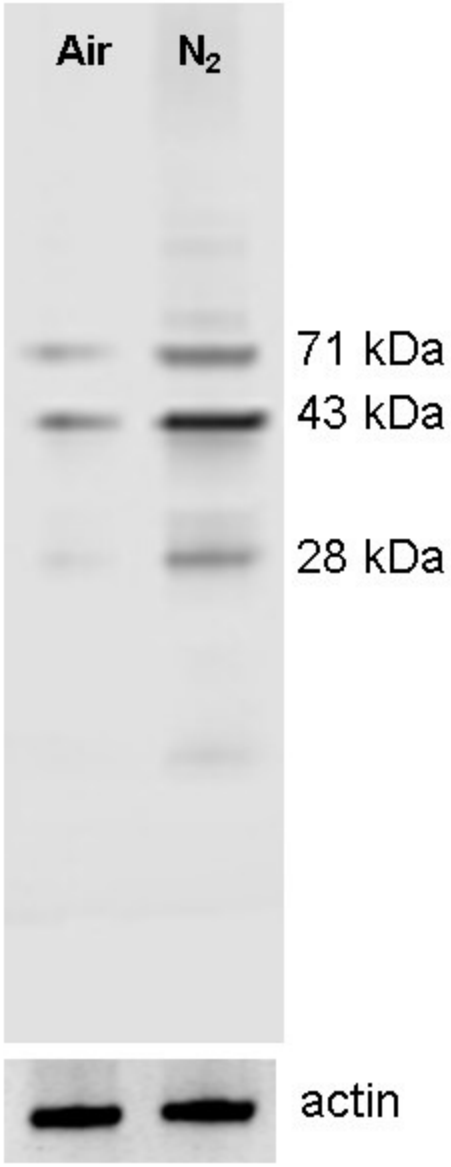

Figure 10

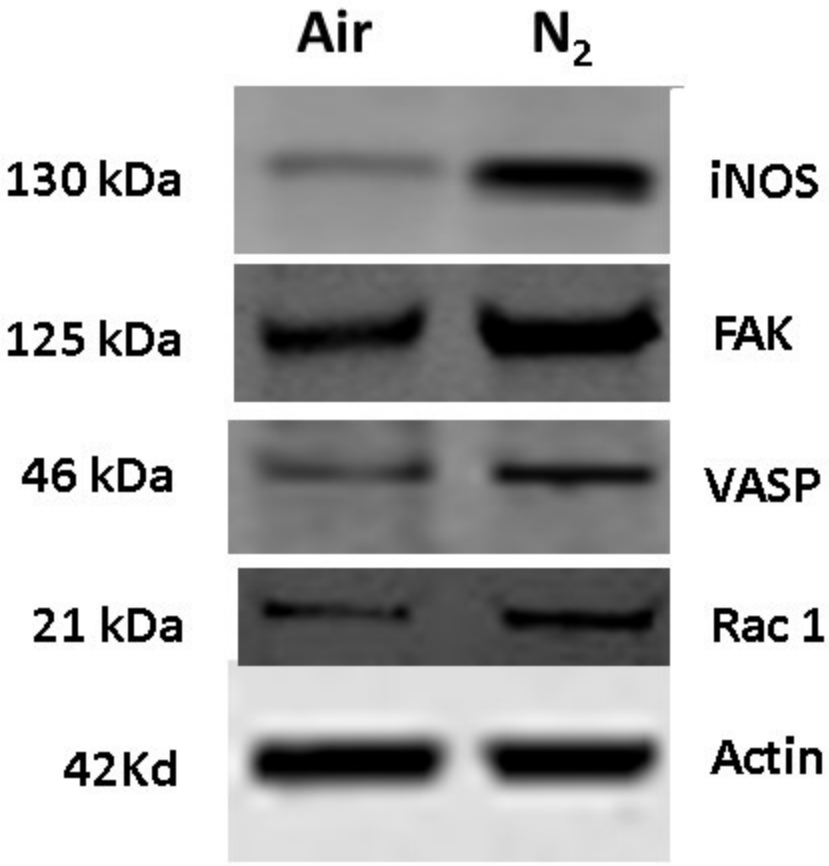
Air
N_2
130 kDa
iNOS
125 kDa
FAK
46 kDa
VASP
21 kDa
Rac 1
42Kd
Actin

Graphical Abstract